J Biol Inorg Chem (2010) 15:919–927
DOI 10.1007/s00775-010-0654-x

ORIGINAL PAPER

Metabolization of $[Ru(\eta^6\text{-}C_6H_5CF_3)(pta)Cl_2]$: a cytotoxic RAPTA-type complex with a strongly electron withdrawing arene ligand

Alexander E. Egger · Christian G. Hartinger · Anna K. Renfrew · Paul J. Dyson

Received: 27 January 2010 / Accepted: 3 March 2010 / Published online: 6 April 2010

Abstract The anticancer ruthenium–arene compound $[Ru(\eta^6\text{-}C_6H_5CF_3)(pta)Cl_2]$ (where pta is 1,3,5-triaza-7-phosphatricyclo[3.3.1.1]decane), termed RAPTA-CF3, with the electron-withdrawing α,α,α-trifluorotoluene ligand, is one of the most cytotoxic RAPTA compounds known. To rationalize the high observed cytotoxicity, the hydrolysis of RAPTA-CF3 in water and brine (100 mM sodium chloride) and its reactions with the protein ubiquitin and a double-stranded oligonucleotide (5′-GTATTGGCACGTA-3′) were studied using NMR spectroscopy, high-resolution Fourier transform ion cyclotron resonance mass spectrometry, and gel electrophoresis. The aquation of the ruthenium–chlorido complex was accompanied by a loss of the arene ligand, independent of the chloride concentration, which is a special property of the compound not observed for other ruthenium–arene complexes with relatively stable ruthenium–arene bonds. Accordingly, the mass spectra of the biomolecule reaction mixtures contained mostly [Ru(pta)]–biomolecule adducts, whereas [Ru(pta)(arene)] adducts typical of other RAPTA compounds were not observed in the protein or DNA binding studies. Gel electrophoresis experiments revealed a significant degree of decomposition of the oligonucleotide, which was more pronounced in the case of RAPTA-CF3 compared with RAPTA-C. Consequently, facile arene loss appears to be responsible for the increased cytotoxicity of RAPTA-CF3.

Keywords Anticancer drugs · Bioorganometallic chemistry · DNA interactions · Mass spectrometry · Protein binding

Introduction

In recent years organometallic compounds have received increased attention as potential anticancer drugs [1, 2]. Different classes of drugs appear to have the potential to overcome the limitations of current chemotherapeutics, including drug resistance, activity in a limited number of tumors, and toxic side effects. Promising compounds include derivatives of the clinically tested titanocene dichloride, ferrocene-modified established drugs, square-planar gold drugs, and ruthenium–arene and osmium–arene complexes [2–5].

Ruthenium coordination compounds are the most prominent non-platinum-based anticancer agents, with two representatives currently undergoing clinical trials [6–8]. The low general toxicity and a mode of action which is supposed to be different from that of established metal-based chemotherapeutics make ruthenium compounds promising drug candidates. The pharmacokinetics upon intravenous administration of the ruthenium(III) complex KP1019 revealed rapid and selective binding to serum proteins, which may prevent ruthenium from being reduced and its subsequent activation in the blood. Hence, activation for reaction with target molecules should only take place in the hypoxic environment of solid tumors,

Electronic supplementary material The online version of this article (doi:10.1007/s00775-010-0654-x) contains supplementary material, which is available to authorized users.

A. E. Egger · C. G. Hartinger · A. K. Renfrew · P. J. Dyson
Institut des Sciences et Ingénierie Chimiques,
Ecole Polytechnique Fédérale de Lausanne (EPFL),
1015 Lausanne, Switzerland

A. E. Egger · C. G. Hartinger (✉)
Institute of Inorganic Chemistry,
University of Vienna, Waehringer Str. 42,
1090 Vienna, Austria
e-mail: christian.hartinger@univie.ac.at

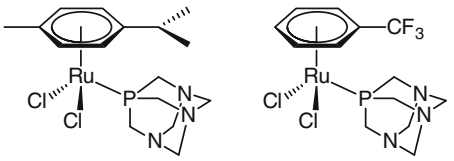

Fig. 1 Structures of RAPTA-C (*left*) and RAPTA-CF3 (*right*)

providing an extra degree of selectivity for diseased tissue over healthy cells [7–9]. The best studied organometallic compounds are based on the ruthenium–arene scaffold and bear monodentate and bidentate ligands [10–18], including halides or dicarboxylates as leaving groups and 1,2-ethylenediamine (en), 1,3,5-triaza-7-phosphatricyclo[3.3.1.1] decane (pta; see Fig. 1 for the structure of the prototype compound RAPTA-C), pyrone, and paullone derivatives, etc. as activity-determining moieties. The ligands surrounding the metal center have a strong impact on the reactivity of the complexes with biological targets, such as DNA and proteins [19]. Notably, variation of the ligand sphere allows the design of compounds with antineoplastic activity against primary tumor or metastasis, as demonstrated recently for en and pta compounds, respectively [11, 14], and for the incorporation of desirable properties such as overcoming drug resistance [20–22]. Most of the ruthenium-based drug candidates mentioned are capable of binding strongly to biological nucleophiles. The reactions of metal complexes bearing halides, mostly chloride, proceed via their replacement with soft donor atoms, such as the imidazole of histidine, the thiol of cysteine, or the thioether of methionine in the case of proteins or with N7 of purine bases, predominantly guanine, in the case of DNA. A multitude of analytical methods have been used to characterize the binding of metal drugs to biomolecules [23–26]. In recent years, mass-spectrometric methods have emerged as leading tools to analyze complex mixtures of biomolecules and metal compounds, especially when coupled with separation methods. These techniques have been used to determine binding kinetics and stability constants, to characterize the adducts formed (including loss of ligands), and to identify drug binding sites [5, 23, 25–37].

Recently, a series of compounds of the general formula [Ru(η^6-fluoroarene)(pta)Cl_2] (fluoroarene is C_6H_5F, $C_6H_5CF_3$, and 1,4-$FC_6H_4CH_3$) was designed with the help of density functional theory calculations, aiming to exploit the pH difference of tumor cells and a healthy environment by modulating the pK_a values [38]; this feature was already successfully used in the case of platinum(II) complexes bearing an aminoalcohol ligand, which can be activated at lower pH for reactivity towards proteins, DNA, and DNA model compounds [7, 39–41]. The α,α,α-trifluorotoluene complex [Ru(η^6-$C_6H_5CF_3$)(pta)Cl_2], termed RAPTA-CF3 (see Fig. 1), was found to be the most cytotoxic in A2780 human ovarian cancer cells, and significantly more cytotoxic than other simple RAPTA compounds.

To establish, at a molecular level, the reason for the increased cytotoxicity of RAPTA-CF3, the hydrolysis and subsequent reactivity of the compound with biomolecules was studied. RAPTA-CF3 was found to be considerably more reactive than RAPTA-C, used as a control in the studies, owing to the facile loss of the α,α,α-trifluorotoluene ligand, and the outcome of these studies are reported herein.

Results and discussion

Metal-based drugs tend to undergo activation following administration and should therefore be considered as prodrugs that are activated in vivo. Such metabolization comprises simple hydrolysis/aquation, which occurs frequently in the case of metallodrugs, and subsequent reaction with proteins, and in the case of platinum complexes, with their ultimate biotarget DNA. In the case of the ruthenium(II)–arene compounds, both the reaction with DNA and that with proteins are considered as potential steps in the modes of action of prominent representatives.

RAPTA complexes have previously been shown to undergo rapid hydrolysis in water through loss of a chlorido ligand [42]. A detailed study of RAPTA-C found that aquation occurs after only seconds, with an equilibrium of 3:1 reached between the dichlorido and monochlorido complexes after 20 min [43]. The hydrolysis product is observed in the $^{31}P\{^1H\}$ NMR spectrum as a second peak, approximately 2 ppm downfield of the peak for the starting compound. The process is suppressed at elevated concentration of chloride such as that found in the bloodstream (100 mM), suggesting that in vivo the drug is activated on reaching the cell, where the concentration is considerably lower (4 mM), in a manner similar to cisplatin [44]. However, it is worth noting that ruthenium–arene compounds can undergo ligand substitution reactions via an arene slippage mechanism and hydrolysis is not a prerequisite for reactivity, and such a mechanism could allow reaction with serum proteins [12].

The $^{31}P\{^1H\}$ NMR spectrum of a freshly prepared solution of RAPTA-CF3 shows a major peak at 30.5 ppm and a peak at −27.5 ppm of low intensity assigned to the hydrolysis product [Ru(η^6-$C_6H_5CF_3$)(H_2O)Cl(pta)]$^+$. When the spectrum is recorded in a solution of 100 mM NaCl, only the peak at 30.5 ppm is observed, suggesting that loss of a chlorido ligand to give [Ru(η^6-$C_6H_5CF_3$)(H_2O)Cl(pta)]$^+$ is inhibited. The stability of RAPTA-CF3 in D_2O was monitored by ^1H and $^{31}P\{^1H\}$ NMR spectroscopy over 72 h. A gradual increase in intensity is observed for the minor peak in the $^{31}P\{^1H\}$

NMR spectra, reaching equilibrium after 24 h at a ratio of 1:2. The aqua product is also observed in the ^{1}H NMR spectra as a second series of peaks approximately 0.1 ppm downfield of the peaks of the original complex. After 5 h, a third peak appears in the $^{31}P\{^{1}H\}$ NMR spectrum at −2.7 ppm, corresponding to uncoordinated, oxidized pta. The formation of this species is concurrent with the presence of free arene in the ^{1}H NMR spectrum at 7.3–7.6 ppm, suggesting that both the arene and pta ligands are released, at least in part, from the resulting ruthenium complex (Fig. 2). The intensity of these peaks increases steadily to reach, after 72 h in solution, an equilibrium of 1:1 with the original complex.

When the study was repeated in the presence of 100 mM NaCl, formation of $[Ru(\eta^6\text{-}C_6H_5CF_3)(H_2O)Cl(pta)]^+$ was not observed; however, peaks corresponding to free arene and oxidized pta were present after only 2 h, and were the major species in solution after 48 h. This behavior is quite different from that of other RAPTA compounds, which are stable for several days in 100 mM NaCl solution and do not generally undergo loss of the arene ligand. The strongly electron withdrawing nature of the $C_6H_5CF_3$ ligand results in a comparatively weak ruthenium–arene bond, and is presumably responsible for the higher cytotoxicity of the complex.

Biomolecule binding studies

To estimate the reactivity of RAPTA-CF3 towards proteins, the ruthenium complex was incubated with the model protein ubiquitin (Ub) at a molar ratio of 2:1 (complex to protein) and the reaction was monitored by analyzing the reaction mixture after 1 and 3 days using electrospray ionization Fourier transform ion cyclotron resonance mass spectrometry (ESI-FT-ICR-MS) in positive ion mode. Prior to flow injection into the mass spectrometer, the sample was diluted 1:100 with a water/acetonitrile/1% formic acid solution, to improve the spraying. The broadband spectra acquired in the range *m/z* 770–870 are shown in Fig. 3 (Ub charge states 11+ and 10+). The spectra are dominated by two main peaks corresponding to unreacted Ub at *m/z* 779.61004 and 857.47032. In addition, in both spectra recorded following incubation with RAPTA-CF3 (at 1 and 3 days) a series of peaks are observed that correspond to adducts of Ub containing fragments of RAPTA-CF3. In contrast to results reported for the structurally similar RAPTA-C [19], the arene ligand is cleaved off in the case of RAPTA-CF3 during the reaction with the protein and mainly adducts of the type $[Ub–Ru(pta)(H_2O)_x]$ ($x = 0$–2) were identified after 1-day reaction (Fig. 3). This result is consistent with the observations during the hydrolysis studies (see earlier). Notably, also an adduct of Ub with solely ruthenium was identified, and in the range *m/z* 790–800 numerous species containing aqua and acetonitrile ligands, which originated from the solution used to improve the spray efficiency, were assigned to *m/z* values. In the *m/z* range 800–810 a series of aqua, acetonitrile, and chloride species were identified. However, several signals overlapped and could not be resolved, although the mass spectra were recorded in high-resolution mode ($R \approx 80{,}000$ at *m/z* 400). After 1-day incubation, the most abundant ruthenium-containing adduct peak was assigned to [Ub + Ru(pta)] with a relative intensity of 28% (Table 1), with regard to the most abundant signal in the spectrum at *m/z* 779.61083, i.e., $[Ub + 11H]^{11+}$. Furthermore, a peak was identified as the metal-free peptide $[^{29}P\cdots G^{76} + 8H]^{8+}$, which might

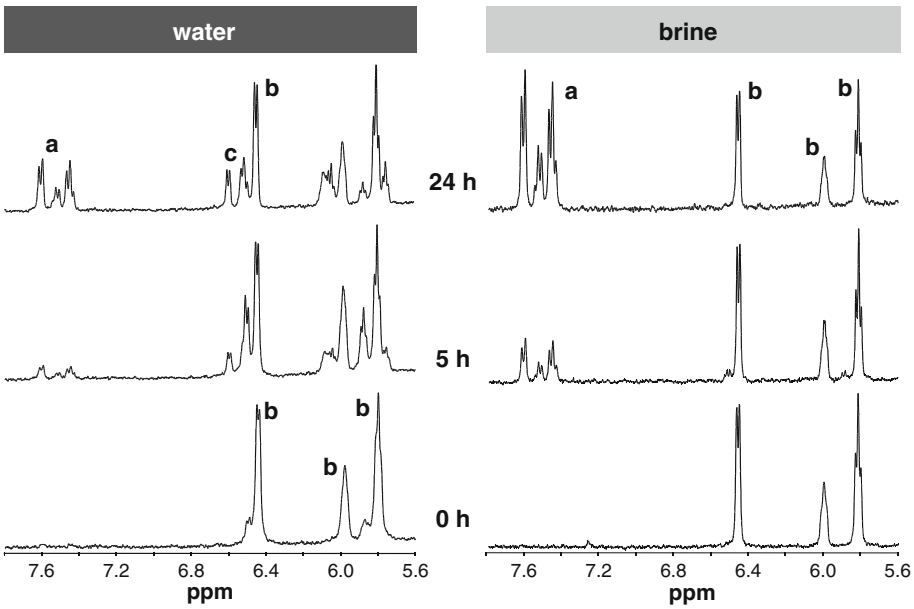

Fig. 2 ^{1}H NMR hydrolysis studies of RAPTA-CF3 in D_2O (*left*) over 24 h, showing that the arene ligand is released over time and aqua species are formed. In brine the degree of arene loss is significantly higher (*right*). Peak assignment: *a* arene, *b* RAPTA-CF3, *c* hydrolysis products

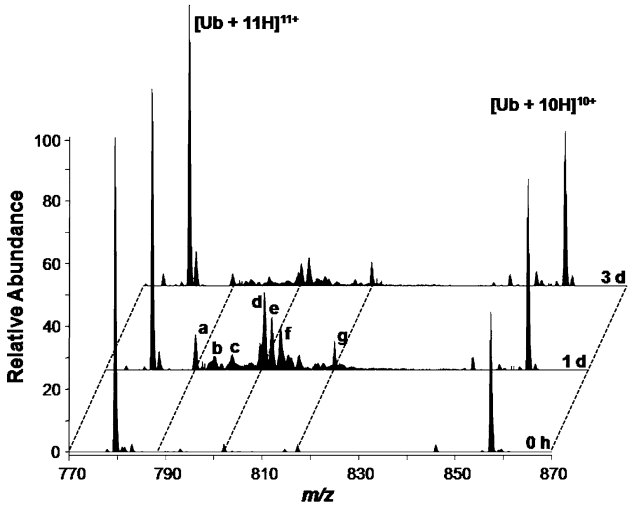

Fig. 3 The reaction of ubiquitin (*Ub*) with RAPTA-CF3 after 0, 24, and 72 h. Peak assignment: *a* $[Ub + Ru + 9H]^{11+}$, *b* $[Ub + Ru(CH_3CN) + 9H]^{11+}$, c $[Ub + Ru(CH_3CN)_2 + 9H]^{11+}$, *d* $[Ub + Ru(pta) + 9H]^{11+}$ (pta is 1,3,5-triaza-7-phosphatricyclo[3.3.1.1] decane), *e* $[Ub + Ru(pta)(H_2O) + 9H]^{11+}$, *f* $[Ub + Ru(pta)Cl + 10H]^{11+}$, *g* $[^{29}P\cdots G^{76} + 8H]^{8+}$

indicate at least partial degradation of the protein. In general the mass accuracy was very good with errors usually 1 ppm or less, enabling exact assignment of a manifold of Ub–Ru species (Table 1). Upon incubation for 3 days, the spectra contained fewer and less abundant adduct peaks compared with incubation for 1 day. $[Ub + 11H]^{11+}$ remained the most abundant peak in the mass spectrum, followed by $[Ub + Ru(pta)(H_2O) + 9H]^{11+}$ (10%) and $[Ub + Ru(pta) + 9H]^{11+}$ (8%).

To evaluate the reactivity of RAPTA-CF3 with DNA, the complex was incubated with a double-stranded 13-mer oligonucleotide (consisting of 5′-GTATTGGCACGTA-3′, S1, and 3′-TACGTGCCAATAC-5′, S1c) at a molar ratio of 1:1 (final DNA concentration 10 μM) in water at 37 °C. Aliquots were taken after 0.25, 1, 3, 9, and 24 h and analyzed by ESI-FT-ICR-MS with respect to adduct formation. Under the spraying conditions applied, the oligonucleotide was separated into its complementary single strands, which were fourfold to eightfold negatively charged and most abundant at charge states 6– and 7–. Hence, only this region is discussed and depicted in Fig. 4. The monoadduct of Ru(pta) with S1c $[S1c + Ru(pta) - 9H]^{7-}$ at *m/z* 595.37471 rapidly became the most prominent peak after incubation for 1 h. At this time, signals corresponding to two Ru(pta) complexes per single strand started to arise and became the second-most abundant peaks after 3 h of incubation. It is noteworthy that all of these adducts are accompanied by a series of aqua adducts (indicated with asterisks in Fig. 4), which were clearest at lower charge states (up to three aqua adducts per DNA strand in case of the $[Ru(pta)]_2$ adduct). Further signals, corresponding to Ru(pta) adducts upon elimination of one adenine or guanine (Fig. 4, indicated with triangles and circles, respectively) from the single-stranded oligonucleotides and consecutive addition of H_2O, were less abundant, but were present throughout the study. These base losses seem to be unspecific as they were also observed in previously published studies with cisplatin under the same conditions [34]. No peaks corresponding to Ru(pta)Cl, Ru(α,α,α-trifluorotoluene)(pta), or Ru(α,α,α-trifluorotoluene)(pta)Cl adducts were observed at any time, indicating quick and complete loss of the arene and chlorido ligands takes place.

Owing to the high resolution of the ion cyclotron resonance technique, isotopic peak patterns were completely resolved and used together with the high-accuracy mass determination for unambiguous identification of the above-mentioned peaks. Figure 5 shows a comparison of the theoretical peak pattern, including the calculated *m/z* value for the most abundant isotopic peak, with the experimental

Table 1 Selected ubiquitin (*Ub*) adducts formed with RAPTA-CF3 and their relative abundances after 1 and 3 days of reaction, observed and theoretical *m/z* values, and the mass accuracy

Identified species	Relative abundance (%)		Theoretical *m/z*	Experimental (1 day) *m/z*	Error (ppm)
	1 day	3 days			
$[Ub + 11H]^{11+}$	100	100	779.61004	779.61083	1.01
$[Ub + Ru + 9H]^{11+}$	13	4	788.59989	788.60007	0.22
$[Ub + Ru(CH_3CN) + 9H]^{11+}$	5	–	792.32958	792.32959	0.01
$[Ub + Ru(CH_3CN)_2 + 9H]^{11+}$	6	3	796.05927	796.05982	0.69
$[Ub + Ru(pta) + 9H]^{11+}$	28	8	802.87962	802.87995	0.41
$[Ub + Ru(pta)(H_2O) + 9H]^{11+}$	19	10	804.51694	804.51650	0.55
$[Ub + Ru(pta)Cl + 10H]^{11+}$	16	–	806.24115	806.24180	0.80
$[^{29}P\cdots G^{76} + 8H]^{8+}$	11	9	817.31944	817.32026	1.00
$[Ub + 10H]^{10+}$	69	55	857.47032	857.47098	0.77

pta 1,3,5-triaza-7-phosphatricyclo[3.3.1.1]decane

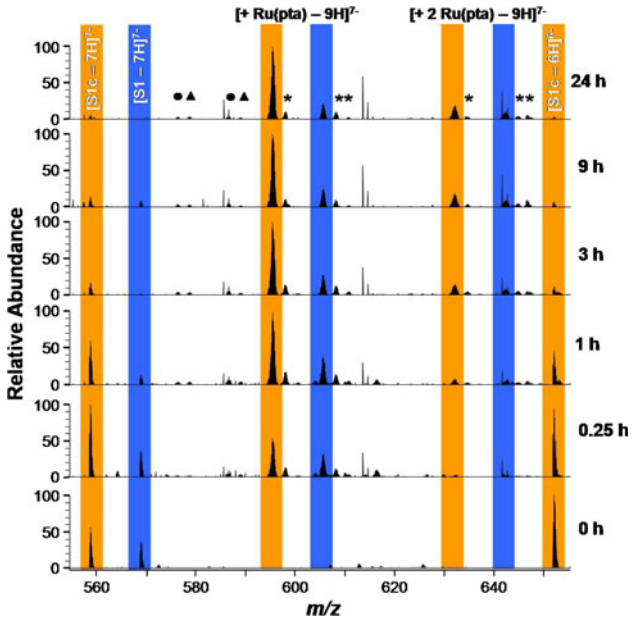

Fig. 4 Charge state 7– of the full-scan mass spectra recorded upon incubation of 10 μM RAPTA-CF3 with an equivalent amount of double-stranded oligonucleotide in water for the time points indicated. Under the ionization conditions applied, strands were detected separately in the mass spectrometer [3′-TACGTGCCAATAC-5′ (S1c) *light gray* and 5′-GTATTGGCACGTA-3′ (S1) *dark gray*]. Adducts of Ru(pta) and $[Ru(pta)]_2$ are formed. *Asterisks* indicate analogous water adducts to the adjacent identified peak. *Triangles* and *circles* indicate [Ru(pta) + H_2O] adducts with loss of adenine or guanine, respectively

pattern for the Ru(pta) and $[Ru(pta)]_2$ adducts, i.e., $[S1c + Ru(pta) - 9H]^{7-}$, $[S1 + Ru(pta) - 9H]^{7-}$, $[S1c + 2\ Ru(pta) - 9H]^{5-}$, and $[S1 + 2\ Ru(pta) - 11H]^{7-}$ at *m/z* 595.37403, 605.51720, 631.94088, and 899.32065. An analogous comparison for the [oligo − B(AH)/B(GH) + Ru(pta) + H_2O] pattern is given in Fig. S1. As the accuracy was typically less than 1 ppm and the peak patterns were identical, accurate assignment of the signals was achievable. Table 2 lists the *m/z* values of the most abundant isotopic peaks of the assigned signals.

The reactivity of RAPTA-C and RAPTA-CF3 with the oligonucleotide was directly compared at drug-to-oligonucleotide ratios of 1:1 and 5:1 upon incubation for 1 and 3 days. For identification of adducts, ESI-FT-ICR-MS was used, and polyacrylamide gel electrophoresis (PAGE) was applied to visualize the structural changes to the DNA (e.g., formation of dimers and degradation of DNA).

Mass spectra of a solution containing a fivefold excess of RAPTA-CF3 or RAPTA-C with the oligonucleotide following incubation for 24 h are depicted in Fig. 6. RAPTA-CF3 preferably releases the two chlorido ligands and the arene ligand, but not the pta ligand, leading to Ru(pta) adducts as described previously. In contrast, RAPTA-C mainly forms Ru(pta)(η^6-*p*-cymene) adducts and only a small amount of oligonucleotide–Ru(pta) was detected, indicating that the introduction of the electron-withdrawing CF_3 group into the arene weakens the ruthenium–arene bond, which is accordingly more easily cleaved off in the case of RAPTA-CF3 compared with the *p*-cymene ligand in RAPTA-C. Consecutively, the vacant positions in the coordination sphere of ruthenium may be occupied by aqua ligands, which explains the series of Ru(pta)$(H_2O)_x$ signals in case of RAPTA-CF3, which do not accompany the Ru(pta)(arene) adduct that is formed in case of RAPTA-C. Hence, the aqua species are unlikely to originate from incomplete desolvatization during electrospray ionization.

Following 3 days of incubation of the oligonucleotide with a fivefold excess of RAPTA-CF3, no peaks that could be readily assigned to the intact oligonucleotide or RAPTA-CF3 modified adducts were observed. Indeed, none of the above-mentioned peaks were observed, indicating that degradation of the oligonucleotide had occurred (as also observed in the case of RAPTA-C). To verify this proposal, reaction mixtures of RAPTA-C and RAPTA-CF3 with

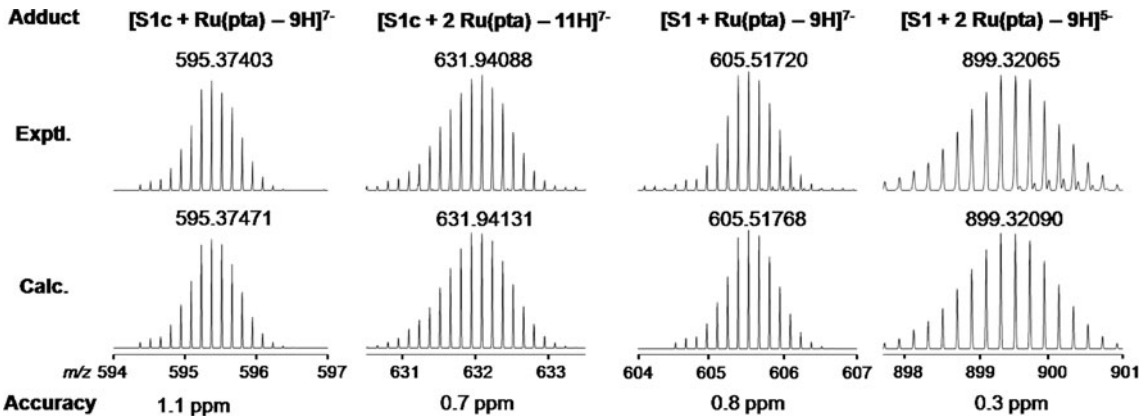

Fig. 5 Comparison of calculated peak patterns with experimental isotopic distributions of selected adducts

Table 2 Selected oligonucleotide adducts formed with RAPTA-CF3

Identified species	Theoretical *m/z*	Experimental *m/z*	Error (ppm)
$[S1c - 7H]^{7-}$	558.66501	558.66495	0.11
$[S1 - 7H]^{7-}$	568.80797	568.80796	0.02
$[S1c - B(GH) + H_2O + Ru(pta) - 9H]^{7-}$	576.36914	576.36840	1.28
$[S1c - B(AH) + H_2O + Ru(pta) - 9H]^{7-}$	578.65415	578.65371	0.76
$[S1 - B(GH) + H_2O + Ru(pta) - 9H]^{7-}$	586.51212	586.51218	0.10
$[S1 - B(AH) + H_2O + Ru(pta) - 9H]^{7-}$	588.79711	588.79695	0.27
$[S1c + Ru(pta) - 9H]^{7-}$	595.37471	595.37403	1.14
$[S1c + Ru(pta)(H_2O) - 9H]^{7-}$	597.94765	597.94695	1.17
$[S1 + Ru(pta) - 9H]^{7-}$	605.51768	605.51720	0.80
$[S1 + Ru(pta)(H_2O) - 9H]^{7-}$	608.09062	608.09024	0.62
$[S1 + Ru(pta)(H_2O)_2 - 9H]^{7-}$	610.66355	610.66295	0.98
$[S1c + 2\ Ru(pta) - 11H]^{7-}$	631.94131	631.94088	0.68
$[S1c + Ru(pta) + Ru(pta)(H_2O) - 11H]^{7-}$	634.51425	634.51347	1.22
$[S1 + 2\ Ru(pta) - 11H]^{7-}$	642.08428	642.08402	0.40
$[S1 + Ru(pta) + Ru(pta)(H_2O) - 11H]^{7-}$	644.65722	644,65664	0.90
$[S1 + 2\ Ru(pta)(H_2O) - 11H]^{7-}$	647.23016	647.23009	0.11
$[S1c - 6H]^{6-}$	651.94372	651.94371	0.02
$[S1 - 6H]^{6-}$	663.77718	663.77726	0.12

S1 5′-GTATTGGCACGTA-3′, *S1c* 3′-TACGTGCCAATAC-5′

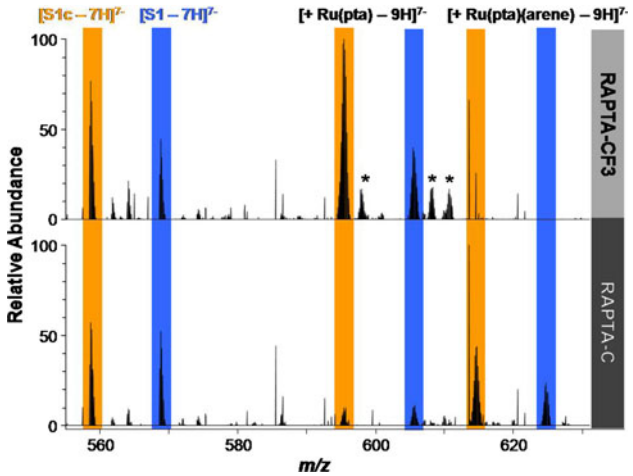

Fig. 6 Comparison of the reaction of RAPTA-CF3 and that of RAPTA-C with a double-stranded oligonucleotide by electrospray ionization mass spectrometry (1 day, ruthenium complex to oligonucleotide ratio 5:1 in water at 37 °C). *Asterisks* indicate water adducts of adjacent identified peaks

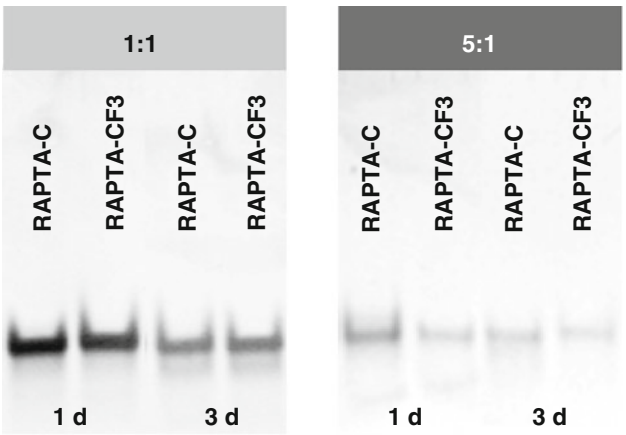

Fig. 7 Gels showing RAPTA-CF3 and RAPTA-C treated oligonucleotide mixtures at incubation ratios of 1:1 and 5:1 following separation

DNA incubated for 1 and 3 days were separated by PAGE (Fig. 7, Table 3). Incubation of DNA with an equimolar amount of complex showed no significant degradation upon 24-h reaction (95 and 90% of intact DNA for RAPTA-C and RAPTA-CF3, respectively), whereas the DNA content upon 3 days of incubation was reduced to approximately 65 and 60%. In the case of a fivefold excess of complex over DNA, degradation was more prominent: in the case of RAPTA-C approximately 30% of DNA was still intact, whereas only approximately less than 10% of DNA was intact in the case of RAPTA-CF3 within 24 h of incubation. Both complexes continued to degrade the DNA, leading to less than 10% of DNA being intact after 3 days of incubation. However, these data should not be considered as absolute values, since ethidium bromide intercalation might be affected by the presence of the complexes.

Table 3 Quantification of DNA degradation in polyacrylamide gel electrophoresis analysis as a function of incubation ratios and time

Complex	Ratio of complex to oligonucleotide	Incubation time (days)	Intact DNA (%)
RAPTA-C	1:1	1	95
		3	65
	5:1	1	30
		3	<10
RAPTA-CF3	1:1	1	90
		3	60
	5:1	1	<10
		3	<10

Conclusions

Ruthenium–arene compounds with a pta ligand, including RAPTA-C as the prototype species, are anticancer drug candidates with notable activity against metastases. RAPTA-CF3 represents a special compound designed with the aim of exploiting one of the different properties of normal and cancer tissues, namely, a significantly lower pH, to achieve higher selectivity in the treatment of cancer [38]. It is noteworthy that RAPTA-CF3 is more cytotoxic than RAPTA-C and other RAPTA compounds. We were able to trace this greater cytotoxicity to the greater reactivity of RAPTA-CF3 over RAPTA-C due to the facile loss of the electron-poor α,α,α-trifluorotoluene ligand.

Hydrolysis studies showed that the α,α,α-trifluorotoluene ligand is released after dissolution in aqueous media. A similar feature was observed in the reactions of RAPTA-CF3 with biomolecules; incubation with the model protein Ub and a short double-stranded oligonucleotide resulted in adduct peaks which are mainly assignable to [Ru(pta)]–biomolecule ions, i.e., with the arene and chlorido ligands cleaved off. The release of the arene ligand allows the formation of rather different biomolecule adducts as compared with classic bifunctional platinum compounds or the parent compound RAPTA-C, with the biomolecule acting as a multidentate ligand. This might have important implications for the mode of action of RAPTA-CF3, as such adducts might resist repair by DNA repair enzymes (should DNA prove to be the target). Furthermore, PAGE studies show that compared with RAPTA-C, RAPTA-CF3 has stronger potential to degrade DNA. In the case of proteins, such multidentate binding might cause significant structural modifications, resulting in altered functions of potential target enzymes.

Materials and methods

RAPTA-C [10] and RAPTA-CF3 [38] were prepared as described previously.

Hydrolysis studies

The hydrolytic stability of RAPTA-CF3 was determined by ^{1}H and $^{31}P\{^{1}H\}$ NMR spectroscopy without light protection. Solutions of RAPTA-CF3 (1 mM) in D_2O (or D_2O containing 100 mM NaCl; pH 5.4–5.8) were incubated at 37 °C over 72 h and aliquots were taken after 0, 0.5, 1, 2, 3, 5, 8, 12, 24, 48, and 72 h. ^{1}H and $^{31}P\{^{1}H\}$ NMR spectra were recorded at 400.13 and 161.98 MHz with a Bruker Avance DPX spectrometer at room temperature using $SiMe_4$ and H_3PO_4 as external standards, respectively.

Protein and (oligo)nucleotide binding studies

Sample preparation

The high performance liquid chromatography purified double-stranded 13-mer oligonucleotide S1 was purchased as an aqueous solution with a concentration of 0.2 mM from A/S Technology (Denmark) and was checked by PAGE for complete annealing. RAPTA-CF3 and RAPTA-C were dissolved in water (200 μM stock solutions) and immediately incubated with the oligonucleotide at effective complex to double-stranded oligonucleotide molar ratios of 1:1 and 5:1 in a total volume of 300 μl in Eppendorf vials (500 μl) in a thermomixer (300 rpm; Eppendorf) at 37 °C. Evaporation was minimized by sealing the tubes with Parafilm® M and covering them with several layers of aluminum foil. To investigate the binding kinetics of RAPTA-CF3, aliquots of 30 μl were taken after 0.25, 1, 3, 9, and 24 h of incubation; for direct comparison of RAPTA-C and RAPTA-CF3, aliquots were taken after 1 and 3 days of incubation. All samples were stored at −20 °C until analysis by mass spectrometry or PAGE.

For mass-spectrometric analysis, the aqueous samples were thawed completely and an aliquot of 10 μl was diluted immediately prior to analysis with 40 μl of a 1.25 mM ammonium acetate solution in 65:10:5 (v/v/v) MeOH/water/1-propanol, resulting in the following final spraying conditions: 2 μM oligonucleotide, 1 mM ammonium acetate, and 65:30:5 MeOH/water/1-propanol.

For the protein binding studies, RAPTA-CF3 was incubated with Ub (from bovine red blood cells, minimum 90%; Sigma) at a molar ratio of 2:1 in water (final protein concentration 100 μM) and samples were taken after 24 and 72 h of incubation at 37 °C. The samples were diluted 1:100 with 70:30:1 (v/v/v) $H_2O/CH_3CN/HCOOH$ and were immediately analyzed by mass spectrometry.

Mass spectrometry

For electrospray ionization mass spectrometry, the samples were placed into a 96-well plate in an Advion TriVersa™

robot (Advion Biosciences, Ithaca, NY, USA) equipped with a 5.5-μm nozzle chip. The electrospray ionization robot was controlled with ChipSoft version 7.2.0 employing the following parameters: for oligonucleotides, gas pressure 0.40 psi, voltage −1.8 to −2.0 kV, sample volume 10 μl, negative ion mode; for protein binding studies, 0.90 psi, voltage 1.4–1.6 kV, sample volume 25 μl, positive ion mode. The samples were analyzed using an ion trap Fourier transform ion cyclotron resonance mass spectrometer comprising an LTQ XL and an 11-T Fourier transform ion cyclotron resonance mass spectrometer (both from Thermo Fisher Scientific, Bremen, Germany). The Xcalibur software bundle (version 2.0.5, Thermo Fischer Scientific) was utilized for data acquisition (Tune Plus version 2.2 SP1; Thermo Fisher Scientific) and data analysis (Qual Browser version 2.2; Thermo Fisher Scientific). Oligonucleotide mass spectra were recorded at a resolution of 75,000 at 500 *m/z* for *m/z* 350–2,000. One scan consisted of five microscans, AGC was set to 1×10^6, the maximum injection time of 500 ms was never exceeded, and the spectrum was averaged over at least 50 scans. The mass spectra were recalibrated using the charge distributions of single-stranded S1c (charge states 4– to 8–). Protein binding data were collected in ion trap (*m/z* 400–2,000), Fourier transform ion cyclotron resonance (*m/z* 400–2,000, resolution of 75,000 at *m/z* 400), and WSIM (*m/z* 770–870; resolution of 40,000 at *m/z* 800) modes. The mass spectra were recalibrated using the 10+ and 11+ charge states of Ub as internal standards in the positive ion mode.

Gel electrophoresis

Samples were thawed and 10-μl aliquots (0.8 μg oligonucleotide) were mixed with 2 μl of 6× sample buffer and completely loaded on a native 20% polyacrylamide gel. Puc-mix (smallest oligonucleotide 45 bp) was used as a mass ruler in the two outermost lanes and pure double-stranded DNA of sequence 5′-GTATTGGCACGTA-3′ (S1) was used in amounts of 0.8, 0.4, and 0.08 μg as standards for estimation of the concentration of the oligonucleotide upon incubation with the metal complexes. Tris(hydroxymethyl)aminomethane–borate–EDTA buffer (1×) was used as electrolyte and electrophoresis was performed at a constant current (12 mA) for 3–4 h. Gels were stained with ethidium bromide (0.5 μg/ml) for 15–20 min and visualized by UV light irradiation. Quantification of DNA bands was performed with ImageJ (National Institutes of Health, USA).

Acknowledgments The authors are indebted to the EPFL, the Swiss National Science Foundation, the University of Vienna, the Austrian Council for Research and Technology Development, and COST D39 and CM0902 for financial support.

References

1. Jaouen G (ed) (2006) Bioorganometallics. Wiley, Weinheim
2. Hartinger CG, Dyson PJ (2009) Chem Soc Rev 38:391–401
3. Nguyen A, Vessieres A, Hillard EA, Top S, Pigeon P, Jaouen G (2007) Chimia 61:716–724
4. Strohfeldt K, Tacke M (2008) Chem Soc Rev 37:1174–1187
5. Casini A, Hartinger CG, Gabbiani C, Mini E, Dyson PJ, Keppler BK, Messori L (2008) J Inorg Biochem 102:564–575
6. Rademaker-Lakhai JM, Van Den Bongard D, Pluim D, Beijnen JH, Schellens JHM (2004) Clin Cancer Res 10:3717–3727
7. Hartinger CG, Zorbas-Seifried S, Jakupec MA, Kynast B, Zorbas H, Keppler BK (2006) J Inorg Biochem 100:891–904
8. Hartinger CG, Jakupec MA, Zorbas-Seifried S, Groessl M, Egger A, Berger W, Zorbas H, Dyson PJ, Keppler BK (2008) Chem Biodivers 5:2140–2155
9. Clarke MJ, Zhu F, Frasca DR (1999) Chem Rev 99:2511–2533
10. Allardyce CS, Dyson PJ, Ellis DJ, Heath SL (2001) Chem Commun 1396–1397
11. Ang WH, Dyson PJ (2006) Eur J Inorg Chem 2006(20):4003–4018
12. Dyson PJ (2007) Chimia 61:698–703
13. Schmid WF, John RO, Mühlgassner G, Heffeter P, Jakupec MA, Galanski M, Berger W, Arion VB, Keppler BK (2007) J Med Chem 50:6343–6355
14. Peacock AFA, Sadler PJ (2008) Chem Asian J 3:1890–1899
15. Mendoza-Ferri MG, Hartinger CG, Eichinger RE, Stolyarova N, Jakupec MA, Nazarov AA, Severin K, Keppler BK (2008) Organometallics 27:2405–2407
16. Mendoza-Ferri MG, Hartinger CG, Mendoza MA, Groessl M, Egger AE, Eichinger RE, Mangrum JB, Farrell NP, Maruszak M, Bednarski PJ, Klein F, Jakupec MA, Nazarov AA, Severin K, Keppler BK (2009) J Med Chem 52:916–925
17. Kandioller W, Hartinger CG, Nazarov AA, Bartel C, Skocic M, Jakupec MA, Arion VB, Keppler BK (2009) Chem Eur J 15:12283–12291
18. Kandioller W, Hartinger CG, Nazarov AA, Kuznetsov ML, John RO, Bartel C, Jakupec MA, Arion VB, Keppler BK (2009) Organometallics 28:4249–4251
19. Scolaro C, Chaplin AB, Hartinger CG, Bergamo A, Cocchietto M, Keppler BK, Sava G, Dyson PJ (2007) Dalton Trans 5065–5072
20. Vock CA, Ang WH, Scolaro C, Phillips AD, Lagopoulos L, Juillerat-Jeanneret L, Sava G, Scopelliti R, Dyson PJ (2007) J Med Chem 50:2166–2175
21. Heffeter P, Jungwirth U, Jakupec M, Hartinger CG, Galanski M, Elbling L, Micksche M, Keppler B, Berger W (2008) Drug Res Update 11:1–16
22. Ang Wee H, Parker Lorien J, De Luca A, Juillerat-Jeanneret L, Morton Craig J, Lo Bello M, Parker Michael W, Dyson Paul J (2009) Angew Chem Int Ed 48:3854–3857
23. Timerbaev AR, Hartinger CG, Aleksenko SS, Keppler BK (2006) Chem Rev 106:2224–2248
24. Hartinger CG, Keppler BK (2007) Electrophoresis 28:3436–3446
25. Groessl M, Hartinger CG, Polec-Pawlak K, Jarosz M, Keppler BK (2008) Electrophoresis 29:2224–2232
26. Hartinger CG, Tsybin YO, Fuchser J, Dyson PJ (2008) Inorg Chem 47:17–19
27. Allardyce CS, Dyson PJ, Coffey J, Johnson N (2002) Rapid Commun Mass Spectrom 16:933–935
28. Pongratz M, Schluga P, Jakupec MA, Arion VB, Hartinger CG, Allmaier G, Keppler BK (2004) J Anal At Spectrom 19:46–51
29. Sulyok M, Hann S, Hartinger CG, Keppler BK, Stingeder G, Koellensperger G (2005) J Anal At Spectrom 20:856–863
30. Khalaila I, Allardyce CS, Verma CS, Dyson PJ (2005) Chembiochem 6:1788–1795

31. Timerbaev AR, Hartinger CG, Keppler BK (2006) Trends Anal Chem 25:868–875
32. Hartinger CG, Ang WH, Casini A, Messori L, Keppler BK, Dyson PJ (2007) J Anal At Spectrom 22:960–967
33. Groessl M, Hartinger CG, Dyson PJ, Keppler BK (2008) J Inorg Biochem 102:1060–1065
34. Egger AE, Hartinger CG, Ben Hamidane H, Tsybin YO, Keppler BK, Dyson PJ (2008) Inorg Chem 47:10626–10633
35. Hartinger CG, Casini A, Duhot C, Tsybin YO, Messori L, Dyson PJ (2008) J Inorg Biochem 102:2136–2141
36. Zhao T, King FL (2009) J Am Soc Mass Spectrom 20:1141–1147
37. Wu Z, Liu Q, Liang X, Yang X, Wang N, Wang X, Sun H, Lu Y, Guo Z (2009) J Biol Inorg Chem 14:1313–1323
38. Renfrew AK, Phillips AD, Tapavicza E, Scopelliti R, Rothlisberger U, Dyson PJ (2009) Organometallics 28:5061–5071
39. Galanski M, Baumgartner C, Meelich K, Arion VB, Fremuth M, Jakupec MA, Schluga P, Hartinger CG, von Keyserlingk NG, Keppler BK (2004) Inorg Chim Acta 357:3237–3244
40. Timerbaev AR, Aleksenko SS, Polec-Pawlak K, Ruzik R, Semenova O, Hartinger CG, Oszwaldowski S, Galanski M, Jarosz M, Keppler BK (2004) Electrophoresis 25:1988–1995
41. Aleksenko SS, Hartinger CG, Semenova O, Meelich K, Timerbaev AR, Keppler BK (2007) J Chromatogr A 1155:218–221
42. Scolaro C, Bergamo A, Brescacin L, Delfino R, Cocchietto M, Laurenczy G, Geldbach TJ, Sava G, Dyson PJ (2005) J Med Chem 48:4161–4171
43. Scolaro C, Hartinger CG, Allardyce CS, Keppler BK, Dyson PJ (2008) J Inorg Biochem 102:1743–1748
44. Hambley TW (2001) J Chem Soc Dalton Trans 2711–2718